

# Generation of Robust Left-Right Asymmetry in the Mouse Embryo Requires a Self-Enhancement and Lateral-Inhibition System

Tetsuya Nakamura,<sup>1,4</sup> Naoki Mine,<sup>1,4,5</sup>  
Etsushi Nakaguchi,<sup>2,4,\*</sup> Atsushi Mochizuki,<sup>3</sup>  
Masamichi Yamamoto,<sup>1</sup> Kenta Yashiro,<sup>1</sup>  
Chikara Meno,<sup>1,6</sup> and Hiroshi Hamada<sup>1,\*</sup>

<sup>1</sup>Developmental Genetics Group  
Graduate School of Frontier Biosciences  
Osaka University and CREST/SORST  
Japan Science and Technology Corporation  
1-3 Yamada-oka

Suita  
Osaka 565-0871  
Japan

<sup>2</sup>Graduate School of Information Science  
Osaka University  
2-1 Yamada-oka  
Suita

Osaka 565-0871  
Japan

<sup>3</sup>Division of Theoretical Biology  
National Institute for Basic Biology  
Okazaki 444-8787  
Japan

## Summary

The bilateral symmetry of the mouse embryo is broken by leftward fluid flow in the node. However, it is unclear how this directional flow is then translated into the robust, left side-specific Nodal gene expression that determines and coordinates left-right situs throughout the embryo. While manipulating *Nodal* and *Lefty* gene expression, we have observed phenomena that are indicative of the involvement of a self-enhancement and lateral-inhibition (SELI) system. We constructed a mathematical SELI model that not only simulates, but also predicts, experimental data. As predicted by the model, *Nodal* expression initiates even on the right side. These results indicate that directional flow represents an initial small difference between the left and right sides of the embryo, but is insufficient to determine embryonic situs. Nodal and Lefty are deployed as a SELI system required to amplify this initial bias and convert it into robust asymmetry.

## Introduction

Nodal and Lefty are members of the transforming growth factor- $\beta$  (TGF- $\beta$ ) family of proteins and play a central role in left-right (L-R) patterning during mouse development (Hamada et al., 2002; Levin, 2005; Tabin,

2005). Nodal functions as a left-side determinant, whereas Lefty functions as a feedback inhibitor of Nodal. Furthermore, Nodal induces both its own synthesis and that of Lefty. We and others (Chen and Schier, 2002; Hamada et al., 2002; Juan and Hamada, 2001; Saijoh et al., 2000) therefore previously suggested that Nodal and Lefty might constitute a reaction-diffusion system, a theoretical model that involves two diffusible molecules, an activator and a feedback inhibitor (Turing, 1952). Since an activator and an inhibitor coexist and diffuse, they can autonomously generate localized patterns. A reaction-diffusion system has been proposed to underlie pattern formation during development because a “self-enhancement and lateral-inhibition” nature of the model can produce “self-organizing patterns” (Meinhardt and Gierer, 2000; Meinhardt, 2001). Importantly, this model has a potential to convert a small difference between two separated regions into a robust difference through local activation and long-range inhibition. Pattern formation events such as skin patterning (Asai et al., 1999; Kondo, 2002) have been explained on the basis of such a system. However, the molecular players remain elusive, and there has been no direct experimental evidence for the operation of such a system in living organisms even though the formation of the *Xenopus* organizers may involve a similar mechanism (Lee et al., 2006).

In the mouse embryo, symmetry breaking for L-R patterning takes place in or around the node. The symmetry-breaking event is the leftward flow of fluid in the node cavity, referred to as nodal flow (Nonaka et al., 1998). An asymmetric signal generated in the node is then thought to be transferred to the lateral plate mesoderm (LPM), where it induces left-sided expression of *Nodal*. It is not clear, however, whether nodal flow alone is sufficient for the generation of robust asymmetry, represented by exclusively left-sided expression of *Nodal* in the LPM. It is thus possible that nodal flow may generate only a small difference between the left and right sides, which is then converted to robust asymmetry by some other mechanism. Given that Lefty and Nodal have the potential to function as a self-enhancement and lateral-inhibition (SELI) system, they may convert a small asymmetry generated by nodal flow into robust asymmetry. We have now tested this possibility by experimental manipulation of mouse embryos and by construction of a mathematical model that is able not only to simulate, but also to predict, developmental events in the mouse embryo.

## Results

### Local Activation and Long-Range Inhibition during L-R Patterning

While studying the role of Nodal in L-R patterning, we observed phenomena that were indicative of the involvement of a SELI system (Figure 1). The introduction by lipofection of a Nodal expression vector into the right LPM of mouse embryos at the early headfold stage (Figure 1A) and subsequent culture of the embryos until

\*Correspondence: nakaguti@ist.osaka-u.ac.jp (E.N.); hamada@fbs.osaka-u.ac.jp (H.H.)

<sup>4</sup>These authors contributed equally to this work.

<sup>5</sup>Present address: Institute for Microbial Diseases, Osaka University, 3-1 Yamada-oka, Suita, Osaka 565-0871, Japan.

<sup>6</sup>Present address: Department of Developmental Biology, Graduate School of Medical Sciences, Kyushu University, Fukuoka 812-8582, Japan.

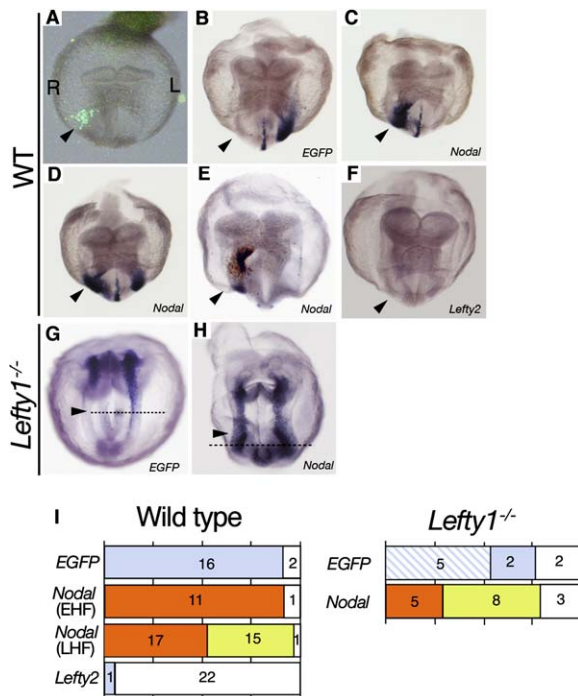


**Figure 1.** Expression of Exogenous *Nodal* on the Right Side Results in Inhibition of Endogenous *Nodal* Expression on the Left Side of Mouse Embryos

(A–H) An EGFP expression vector either (A, B, and G) alone or together with an expression vector for (C–E and G–I) *Nodal* or for (F) *Lefty2* was introduced into the right LPM of (A–F) wild-type or (G and H) *Lefty1*<sup>-/-</sup> mouse embryos. Vectors were introduced at the early headfold stage, with the exception of the embryo in (D), which was injected at the late headfold stage. Transfected embryos were cultured for 12 hr and then subjected to one- or two-color whole-mount in situ hybridization with *Nodal* plus either (B–D and F–H) *Lefty1* or (E) *Lefty2* probes, respectively. The blue and red hybridization signals in (E) indicate *Nodal* and *Lefty2* expression, respectively. (A) Successful transfection was verified for each embryo by the detection of EGFP fluorescence. Embryos in (G) and (H) are viewed from the distal side; all other embryos are viewed from the anterior side. Arrowheads indicate the site of injection with expression vectors.

(I) Summary of the effects of the indicated expression vectors introduced into the right LPM of wild-type or *Lefty1*<sup>-/-</sup> embryos on *Nodal* expression. Blue, left-sided expression; red, right-sided expression; green, bilateral expression; blue stripes, bilateral expression in the anterior portion, but left-sided expression in the remaining region; white, no expression. The numbers of embryos showing each pattern are indicated within the bars. EHF, early headfold stage; LHF, late headfold stage.

they had developed to the five- to six-somite stage thus resulted not only in robust *Nodal* expression in the right LPM, but also in inhibition of *Nodal* expression that would normally have occurred (~12 hr later) in the left LPM (Figures 1C and 1I). This effect depended on the stage at which the *Nodal* expression vector was introduced into the right LPM, with the later the introduction, the less effective the suppression of *Nodal* expression on the left side (Figures 1D and 1I). *Nodal* expression in the left LPM remained absent even when the treated embryos were incubated until the nine-somite stage (data not shown), indicative of highly effective inhibition. Introduction of a control vector for enhanced green fluorescent protein (EGFP) did not affect the normal expression of *Nodal* in the left LPM (Figures 1B and 1I).

The repression of *Nodal* expression on the left side induced by expression on the right side suggested the operation of a SELI system. Indeed, the repression of *Nodal* expression on the left side was found to involve *Lefty*. The ectopic expression of both *Lefty1* and *Lefty2* was thus also induced on the right side in response to injection of the *Nodal* expression vector into the right LPM (Figures 1C and 1E). In *Lefty1*<sup>-/-</sup> embryos, asymmetric expression of *Nodal* begins normally (Figure 1G), but expression subsequently appears in the anterior portion of the right LPM (Meno et al., 1998). However, lipofection of the *Nodal* expression vector into the right LPM of *Lefty1*<sup>-/-</sup> embryos did not efficiently inhibit the subsequent expression of *Nodal* on the left side (Figures 1H and 1I).

If a SELI system operates, *Nodal* expression would be induced in the right LPM when the left LPM is removed or inactivated (because the right LPM would be primed for activation in the absence of inhibition from the left side). We therefore dissected the right LPM, with or without the node, from wild-type mouse embryos at the two-somite stage (Figure 2A). The explants were cultured for 6 hr and then examined for *Nodal* expression. Node cilia of the right LPM-node explants were observed during culture and were found to be motile even at the end of the culture period (data not shown). For explants that included the node, the right LPM expressed *Nodal* in three of seven instances (Figures 2C and 2D). However, *Nodal* expression was absent in the right LPM for all explants that lacked the node (Figures 2B and 2D), suggesting that the activating signal from the node is necessary for the induction of *Nodal* expression in the dissected right LPM.

We further tested our predictions with a different experimental system. Inhibition of *Nodal* expression in the left LPM would be expected to result in right-sided or bilateral expression of *Nodal* in the LPM depending on the level of inhibition (complete or partial inhibition resulting in right-sided or bilateral expression, respectively). Among various agents tested for their ability to inhibit *Nodal* expression in the left LPM, we found an expression vector for an EGFP-*Lefty2* fusion protein to be the most useful (Figures 2G–2K). Introduction of the EGFP-*Lefty2* vector at a low concentration (40 ng/μl) into the left LPM indeed resulted in bilateral or right-sided expression of *Nodal* in some of the injected embryos (Figures 2G, 2H, and 2K). Similar results were obtained for expression of *Pitx2* (Figures 2I, 2J, and 2K), which is also responsive to *Nodal* signaling (Shiratori et al., 2001). The effects of right-sided activation (Figure 1) and left-sided inhibition (Figure 2) thus demonstrate communication between the two sides of the LPM and suggest the involvement of a SELI system. These observations indicate that the right LPM does indeed receive an activating signal, albeit at a lower level than that received by the left LPM. In normal embryos, *Nodal* expression in the right LPM is repressed by the inhibitors *Lefty1* and *Lefty2*, which are produced on the left side.

#### Construction of a Mathematical Model and Analysis of Its General Behavior

These results prompted us to construct a mathematical model for L-R patterning, which is similar to an activator-inhibitor model proposed by Meinhardt (2001).

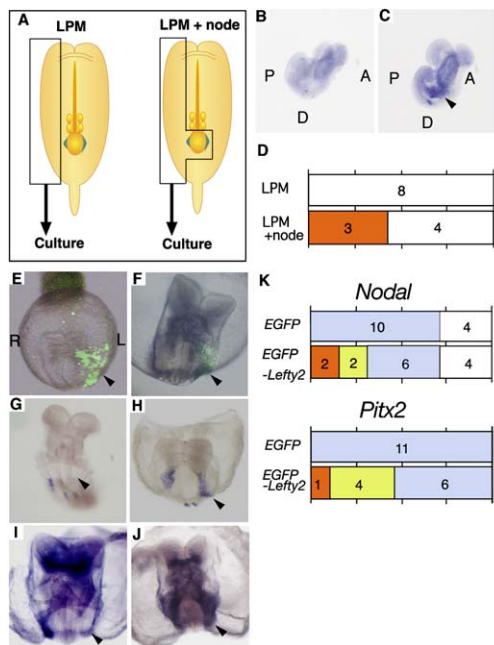


Figure 2. Suppression of the Left Side Results in Activation of the Right Side in Mouse Embryos

(A) Experimental strategy for explant culture. The right LPM with or without the node was dissected from mouse embryos at the two-somite stage and cultured. Blue shading indicates *Nodal* expression around the node.

(B and C) Explants viewed from the left side after in situ hybridization with a *Nodal* probe. *Nodal* expression (arrowhead) was induced in (C) the right LPM with the node, but not in (B) the right LPM without the node. D, distal side of the explants.

(D) Summary of the results of explant experiments. The color code for *Nodal* expression is as in Figure 11.

(E–J) An expression vector for (E and F) EGFP or for an (G–J) EGFP-Lefty2 fusion protein was introduced into a wide region of the left LPM of wild-type mouse embryos at the early headfold stage. After culture for (E, G, and H) 12 hr or (F, I, and J) 16 hr, the transfected embryos were subjected to whole-mount in situ hybridization with (G and H) *Nodal* or (I and J) *Pitx2* probes. EGFP fluorescence images of embryos are shown in (E) and (F). Representative embryos exhibiting (G and I) right-sided or (H and J) bilateral expression are shown. All embryos are viewed from the anterior side. Arrowheads indicate the site of vector injection.

(K) Summary of expression patterns for *Nodal* and *Pitx2* in embryos injected on the left side with EGFP or EGFP-Lefty2 expression vectors. The color code is as in Figure 11.

In particular, we constructed a SELI model, which is defined by regulatory interactions between *Nodal* and *Lefty*: *Nodal* induces synthesis of *Nodal* itself and that of a feedback inhibitor, *Lefty*, both of which can diffuse (Figure 3A). In addition, synthesis of *Nodal* and *Lefty* is induced by the same signaling cascade (Figure 3A) that includes ActR II, Alk4, EGF-CFC, Smad, and FoxH1 (Hamada et al., 2002).

We first generated a space-free model to understand the qualitative behavior of the *Nodal* and *Lefty* dynamics (mathematical formulation of this model is described in the Supplemental Data available with this article online). The model is formally analogous to other types of feedback-enhanced systems in biology, such as the neural action potential. Depending on parameter conditions, several different patterns of dynamics arise from the model: “signal-dependent amplification” patterns (Fig-

ure 3B; Figure S2A; see the Supplemental Data), “bi-stable” patterns (Figures S2B and S2C), and “stable at the origin” patterns (Figure S2D). For instance, the signal-dependent amplification pattern shown in Figure 3B appears only when the degradation rate of *Nodal* is sufficiently faster than that of *Lefty* and the *Nodal*-mediated self-induction rate is larger than the *Lefty*-mediated repression rate (Supplemental Data). Among these patterns, the signal-dependent amplification pattern (shown in Figure 3B) matches the dynamics that are observed in the mouse embryo. Thus, when the initial level of *Nodal* ( $N_i$ ) is large enough (as in the left LPM), the levels of *Nodal* ( $N$ ) and *Lefty* ( $L$ ) will transiently increase, subsequently decrease, and finally converge to zero (dynamics ② shown by the blue arrow, Figure 3B). However, when  $N_i$  is small (as in the right LPM),  $N$  and  $L$  would converge to zero without increasing (dynamics ① shown by the red arrow, Figure 3B). In various L-R mutant mice, *Nodal* expression may be left, right, bilateral, or may be absent (none), which can be explained by the qualitative behavior of the signal-dependent amplification pattern shown in Figure 3B. Thus, when  $N_i$  is large enough on both sides, the “transient increase followed by decrease” dynamics (dynamics ②, Figure 3B) would appear on both sides, resulting in a bilateral phenotype (Figure 3C). When  $N_i$  is too small on both sides, the “converge to zero without increase” dynamics (dynamics ①, Figure 3B) would arise on both sides. Therefore, the signal-dependent amplification pattern (Figure 3B) can give rise to left, right, bilateral, and none phenotypes, depending on the size of  $N_i$  on each side.

To analyze the mechanism of L-R patterning more precisely, we next integrated special terms into the SELI model (Supplemental Data; Figures S2E and S2F) and performed a computer simulation (Figures 3F and 3G; Figure S3). Given that asymmetric *Nodal* expression in the LPM begins in the region adjacent to the node (Figure S1), we designed a one-dimensional SELI system model (Figure 3D; Supplemental Data) that would simulate how *Nodal* expression begins and changes at three locations (the midline, the left LPM, and the right LPM) at the level of the node (the level indicated by the dotted lines in Figure 3E and Figure S1B). Because the model is only one-dimensional, it does not simulate how *Nodal* expression expands within the LPM along the anteroposterior axis. This simulation model could simulate the existing data on the expression patterns of *Nodal*, *Lefty1*, *Lefty2*, and *Pitx2* (the expression of which is also activated by *Nodal*) in wild-type embryos (Figure 3F) as well as in various L-R patterning mutants (Figure S3). The diffusion rates of the activator and inhibitor are important parameters of a SELI system. In principle, such a system requires that both the activator and inhibitor are able to diffuse over large distances and that the inhibitor spreads more efficiently than the activator.

*Nodal* activity indeed travels over a large distance (Chen and Schier, 2001; Meno et al., 2001). *Lefty* also exerts its function over a large distance, given that expression of exogenous *Lefty2* in the right LPM at the early headfold stage prevented endogenous *Nodal* expression in the left LPM (Figures 1F and 1I). We next examined whether *Lefty* activity spreads farther than does *Nodal* activity (Figures 4A and 4B). Introduction of a *Nodal* expression vector into a small region of the

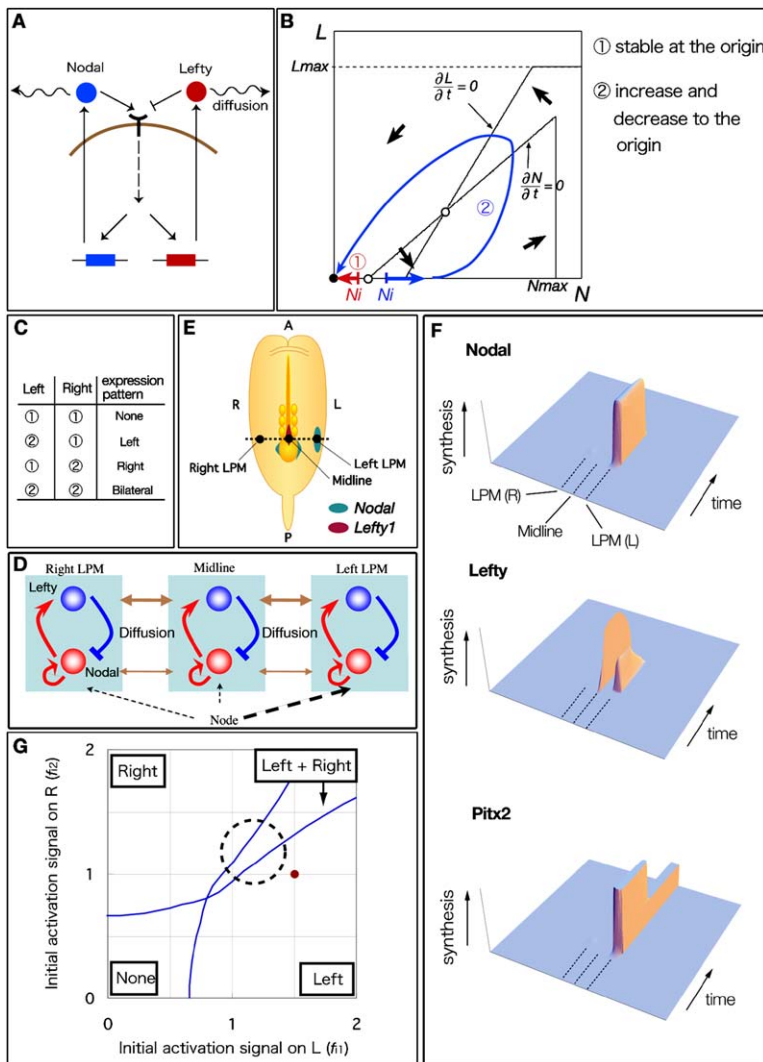


Figure 3. Mathematical Model of L-R Patterning in the Mouse Embryo

(A) Interactions between two diffusible molecules, Nodal (activator) and Lefty (feedback inhibitor). Synthesis of Nodal and Lefty is induced by the same Nodal signaling pathway. (B) Qualitative behavior of the model. Among several different patterns of dynamics that can arise from the mathematical model (described in “Qualitative Behavior of the Model” in Supplemental Data), the one that matches the in vivo dynamics is shown here, while other possible patterns are shown in Figure S2.  $L$ , the level of Lefty;  $N$ , the level of Nodal;  $N_i$ , the initial level of Nodal. When  $N_i$  is large enough (the blue vertical bar),  $N$  and  $L$  would show a “transient increase followed by decrease” dynamics (dynamics ② shown by the blue arrow and blue line). When  $N_i$  is small (the red vertical bar),  $N$  and  $L$  would show a “converge to zero without increase” dynamics (dynamics ① shown by the red arrow). Black and white circles indicate stable and unstable equilibrium points, respectively. Bold, black arrows are vector-field representations of dynamics in each area.

(C) Theoretical understanding of L-R mutant phenotype. ① and ② indicate two different dynamics shown in (B), a “converge to zero without increase” dynamics and a “transient increase followed by decrease” dynamics, respectively. The phenotype of a mutant can be explained by combinations of ① and ②. Thus, depending on the level of  $N_i$  on each side, *Nodal* expression can be left sided, right sided, bilateral, or absent.

(D) Basis of simulations by the mathematical model. The initial activating signal ( $f_i$ ) derived from the node (dotted lines) activates *Nodal* and *Lefty* expression at the midline and in the LPM by the positive loop (red arrows). The *Lefty* protein thus produced inhibits *Nodal* expression by the negative loop (blue lines). *Nodal* protein (red circles) and *Lefty* protein (blue circles) diffuse in both directions (brown arrows).

(E) Topology of the mouse embryo at the stage selected for simulation. The model is designed to simulate how *Nodal* expression begins and changes at three locations: the midline, the left LPM, and the right LPM at the level of the node (indicated by the dotted line). A, anterior; P, posterior.

(F) Simulation by the mathematical model of L-R asymmetric expression of *Nodal*, *Lefty*, and *Pitx2* in wild-type embryos, showing how expression of each gene at the three locations changes.

(G) Relationship between *Nodal* expression patterns in the LPM and the levels of the initial activating signal in the left ( $f_{l1}$ ) and right ( $f_{r1}$ ) LPM. Depending on the values of  $f_{l1}$  and  $f_{r1}$ , *Nodal* expression in the LPM may be either left sided, right sided, bilateral, or absent. The blue lines indicate borders between different expression patterns. The estimated values of  $f_{l1}$  and  $f_{r1}$  for wild-type embryos are indicated by the red dot. In *iv/iv* embryos,  $f_{l1}$  and  $f_{r1}$  fluctuate within the area indicated by the broken circle.

yolk sac near the right LPM resulted in diffusion of Nodal protein produced there to the LPM, where it activated the endogenous *Nodal* gene (Figures 4C, 4D, and 4I). However, introduction of a *Lefty1* or *Lefty2* expression vector in a separate and more distant region blocked the *Nodal* expression in the LPM induced by introduction of the *Nodal* expression vector in all embryos tested (Figures 4E–4I). A similar level of *Lefty* expression, even at a distance from the LPM three times that of the ectopic *Nodal* expression, efficiently blocked *Nodal* expression in the LPM (Figures 4F and 4H). These results thus suggested that *Lefty* activity spreads farther than *Nodal* activity.

In the model, the L-R pattern of gene expression in the LPM depends on the level of the initial activating signal

( $f_i$ ) on both sides of the LPM (Figure 3G). If  $f_i$  on the left ( $f_{l1}$ ) is sufficiently larger than  $f_i$  on the right ( $f_{r1}$ ), then the normal L-R pattern of gene expression ensues. If the difference between  $f_{l1}$  and  $f_{r1}$  is too small, then *Nodal* is expressed bilaterally. In *iv* mutant mice, which possess immotile cilia (Lowe et al., 1996; Okada et al., 1999; Supp et al., 1997), the  $f_i$  values for the two sides likely differ only slightly, but fluctuate within a broad range (Figure 3G), with the result that three different L-R patterns of gene expression can develop in the LPM (Figures S3E–S3G). The model also predicts that a relatively small difference between  $f_{l1}$  and  $f_{r1}$  (for example, values of 1.5 versus 1.0, respectively) would be sufficient to generate robust asymmetry in the LPM (a red dot shown in Figure 3G).

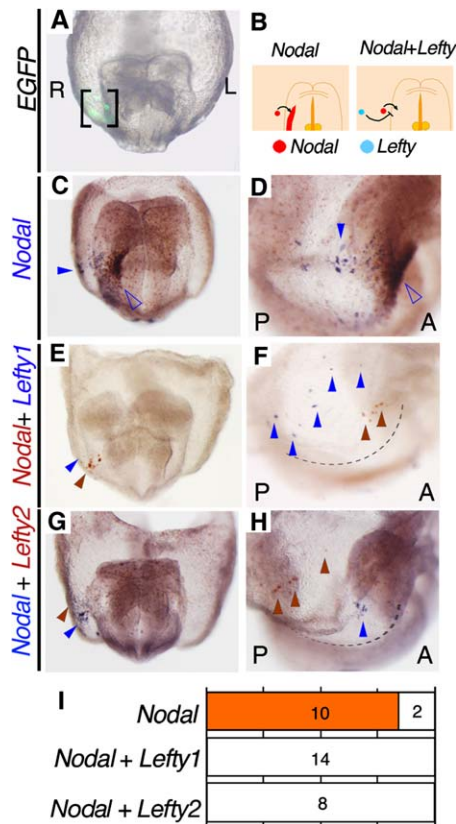


**Figure 4. Lefty Activity Diffuses Farther than Nodal Activity**  
(A and B) Experimental strategy. Expression vectors for Nodal and Lefty were separately introduced into the yolk sac near the right LPM of wild-type embryos at the early headfold stage. The sites of injection are indicated in the fluorescence image of EGFP derived from a cotransfected vector in (A). If Lefty diffuses more efficiently than Nodal, the induction of endogenous *Nodal* expression by exogenous Lefty generated at a transfection site located more distant than that for the Nodal vector, as represented in (B).  
(C and D) Expression of exogenous *Nodal* in the yolk sac (closed arrowheads) induced endogenous *Nodal* expression in the LPM (open arrowheads).  
(E–H) Expression of exogenous (E and F) *Lefty1* or (G and H) *Lefty2* in the yolk sac at a site more distant than that of exogenous *Nodal* expression inhibited the induction of endogenous *Nodal* expression in the LPM. Lipofected expression vectors are indicated on the left, and whole-mount in situ hybridization was performed with the corresponding probes. The positions of the right LPM in (F) and (H) are indicated by the dotted lines. Colors of the vector names and arrowheads correspond to the developed colors in the embryos. Embryos in (D), (F), and (H) are the same as those in (C), (E), and (G), respectively.  
(I) Summary of the experimental results. The numbers of embryos examined are indicated. Red, endogenous *Nodal* expression in the right LPM; white, no endogenous *Nodal* expression.

**Explanation of Unpredictable L-R Phenotypes by the Model**

In addition to being able to simulate existing data on the expression patterns of *Nodal*, *Lefty1*, and *Lefty2* in various L-R patterning mutants (Figure S3), the model provides a mechanistic basis for unexpected observations. We have previously studied the role of the transcription factor FoxH1 in L-R patterning by conditional deletion of *Foxh1* through LPM-specific expression of the Cre

recombinase (Yamamoto et al., 2003). In many (19/34) of the embryos in which deletion of *Foxh1* was efficient, expression of left side-specific genes such as *Nodal* and *Pitx2* was lost. However, in the remaining (15/34) embryos in which deletion of *Foxh1* occurred in a mosaic pattern, a low level of *Pitx2* expression was apparent (Figure 5I). In some of these embryos, however, *Pitx2* expression was bilateral (Figures 5D, 5F, and 5I). This unexpected observation can be readily explained by the SELI model.

In response to the Nodal signal, FoxH1 induces the expression of *Nodal* and *Lefty* (Saijoh et al., 2000; Whitman, 1998). Our model predicts that the level of the Cre-mediated deletion greatly influences the *Pitx2* expression pattern (Figures 5A and 5B). If the *FoxH1* gene is deleted in 50% of LPM cells, *Pitx2* expression in the LPM would remain left sided (Figure 5B), which is represented by 10 of the 34 *Foxh1* conditional mutant embryos (Figures 5H and 5I). If the *FoxH1* gene is deleted in 90% of LPM cells, the model predicts that *Pitx2* expression will be bilateral (Figure 5B), which was the outcome in 5 of the 34 *Foxh1* conditional mutant embryos (Figures 5D, 5F, and 5I). The model is thus able to explain the phenotype of *Foxh1* conditional knockout mice, which is otherwise difficult to understand.

**Both Lefty1 and Lefty2 Contribute to the Generation of Robust Asymmetry**

In the *Lefty1*<sup>-/-</sup> and *Lefty2*<sup>ΔASE/ΔASE</sup> mutants, expression of *Nodal* is initially asymmetric, although it subsequently becomes bilateral as a result of the leakage of Nodal activity toward the right side; right-sided *Nodal* expression is confined to the anterior or posterior portion of the LPM, respectively, and is absent at the level of the node (Figures 1G, 1I, 6D, and 6E) (Meno et al., 1998, 2001). Thus, the normal L-R pattern of *Nodal* expression in the LPM can be initially established in the absence of *Lefty1* or *Lefty2*. However, our model predicts that the roles of *Lefty1* and *Lefty2* would become apparent if *f<sub>i</sub>* were altered (that is, if nodal flow were lost). To test this prediction, we prepared *iv/iv*, *Lefty1*<sup>-/-</sup> and *iv/iv*, *Lefty2*<sup>ΔASE/ΔASE</sup> double mutant embryos and examined them for *Nodal* expression. As predicted by our model (Figure 6L), *Nodal* expression was initiated bilaterally in most *iv/iv*, *Lefty1*<sup>-/-</sup> mice (Figures 6F, 6G, and 6J). In addition, the frequency of bilateral initiation of *Nodal* expression was increased in *iv/iv*, *Lefty2*<sup>ΔASE/ΔASE</sup> mice (Figures 6H, 6I, and 6K). The frequency of bilateral initiation of *Nodal* expression was slightly higher in *iv/iv*, *Lefty1*<sup>-/-</sup> embryos than in *iv/iv*, *Lefty2*<sup>ΔASE/ΔASE</sup> embryos, suggesting that both *Lefty1* and *Lefty2* contribute to asymmetric initiation of *Nodal* expression in the LPM, but that the contribution of *Lefty1* may be greater than that of *Lefty2*.

Mutant mice deficient in components of intraflagellar transport such as *Polaris*, *KIF3*, and *Wim* lack node cilia (and nodal flow) and exhibit bilateral *Nodal* or *Lefty2* expression (Huangfu et al., 2003; Murcia et al., 2000; Nonaka et al., 1998), in contrast to *iv/iv* embryos, which have immotile cilia and show randomized *Nodal* expression in the LPM. However, such intraflagellar transport mutants are similar to the *iv/iv*, *Lefty1*<sup>-/-</sup> mouse in that they also lack *Lefty1* expression at the midline (our unpublished data). The phenotype of intraflagellar transport mutants

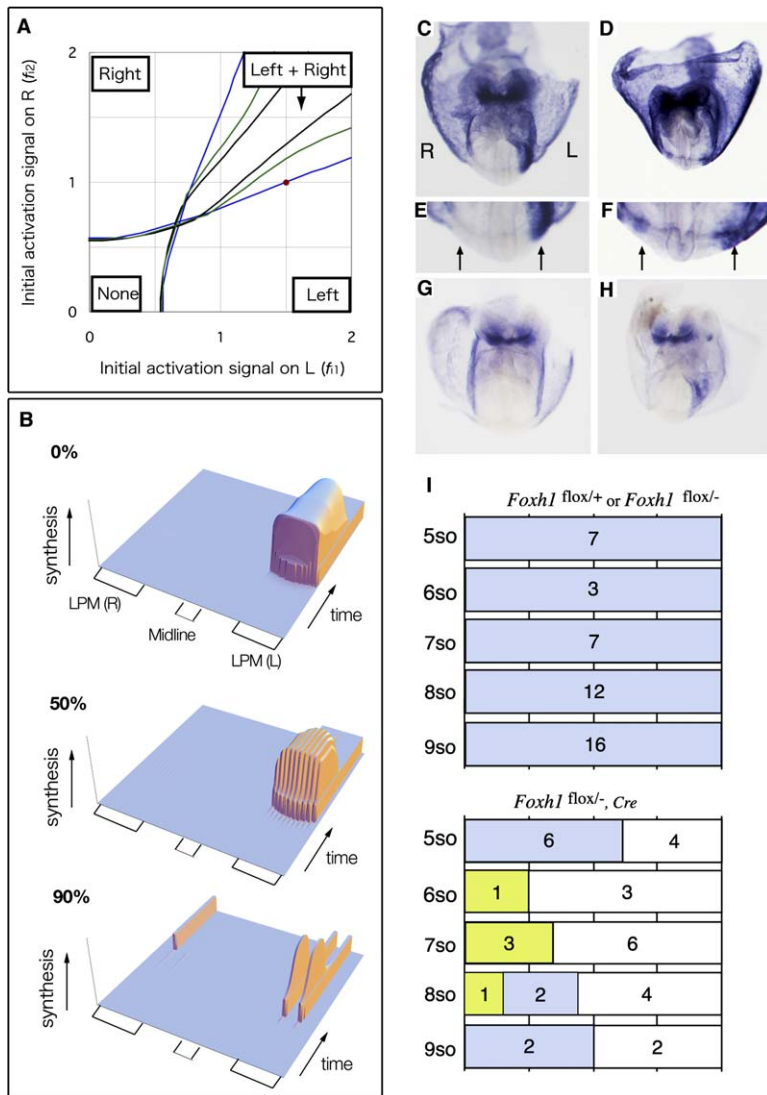


Figure 5. The Model Explains an Unpredicted L-R Phenotype of *Foxh1* Mutant Embryos

(A) Relationship between *Pitx2* expression patterns in the LPM and the levels of the initial activation signal in the left ( $f_{1l}$ ) and right ( $f_{1r}$ ) LPM. The black, green, and blue lines indicate borders of different expression patterns when the degree of Cre-mediated deletion of the *Foxh1* gene is 0% (the value used for the wild-type), 50%, or 90%, respectively. Similar patterns are obtained for *Nodal* expression (data not shown).

(B) Simulation of *Pitx2* expression with various levels of the Cre-mediated deletion (0%, 50%, and 90%).

(C–H) *Pitx2* expression in (C and E) *Foxh1*<sup>flox/+</sup> and (D, F, G, and H) *Foxh1*<sup>flox/-</sup>, *Cre* embryos at the ~6- to 7-somite stage; the latter embryos express Cre recombinase specifically in the LPM. The distal regions of the embryos in (C) and (D) are shown at higher magnification in (E) and (F), respectively. Arrows indicate the LPM positive for *Pitx2* expression. An embryo in (G) has no expression, and that in (H) has left-sided expression.

(I) Summary of expression patterns for *Pitx2* in *Foxh1*<sup>flox/+</sup> or *Foxh1*<sup>flox/-</sup> (top) and *Foxh1*<sup>flox/-</sup>, *Cre* (bottom) embryos at the indicated stages (so, somite). The color code is as in Figure 1I.

can thus be simulated by the absence of nodal flow and a lack of *Lefty1* and *Lefty2* in the midline (Supplemental Data; Figure S3K).

#### The Right Side also Receives an Activating Signal, but at a Level Lower Than that on the Left Side

Our model predicts that a small difference in the level of the initial activating signal between the left and right sides of the LPM is sufficient to generate robust L-R asymmetry in gene expression. The right LPM thus also receives the initial activating signal, albeit at a level lower than that of the signal received by the left side. If the activating signal arrives at the right LPM as well as at the left LPM, then *Nodal* expression might be initiated in the right LPM, amplified to a certain level, and then terminated by long-range inhibition from the left side. Indeed, our model predicts that *Nodal* is expressed transiently and at a low level in the right LPM (Figure 7A). Although *Nodal* mRNA has not been detected in the right LPM by conventional in situ hybridization, we were able to detect *Nodal* mRNA in the right LPM by reverse transcription (RT) and by polymerase chain reaction (PCR).

A piece of the left LPM or the right LPM at the level of the node was dissected from embryos at the two- to six-somite stages (Figure 7B), and RNA was prepared from each LPM specimen. Care was taken to avoid crosscontamination between left and right LPM tissue. We were also careful not to include the node, in which *Nodal* is expressed; indeed, we examined each RNA preparation for the presence of transcripts of *L-Plunc*, which is expressed in the node, but not in the LPM (Hou et al., 2004). Most of the RNA samples were negative for *L-Plunc* mRNA (Figure 7C), and these samples were then examined for transcripts of *Nodal* and *Lefty2* (Figures 7C and 7D). The results obtained with 27 pairs of LPM specimens are summarized in Figure 7D; the amounts of PCR products for *Nodal* or *Lefty2* were normalized by that of the product for *HPRT*. As predicted by the model, *Nodal* mRNA was detected in the right LPM in a stage-dependent manner. At the three-somite stage, *Nodal* mRNA was detected in the left LPM, but was absent in the right LPM. At the four- and five-somite stages, when *Nodal* expression is maximal and detected exclusively in the left LPM by in situ hybridization, *Nodal* mRNA was detected by RT-PCR in all samples of the left

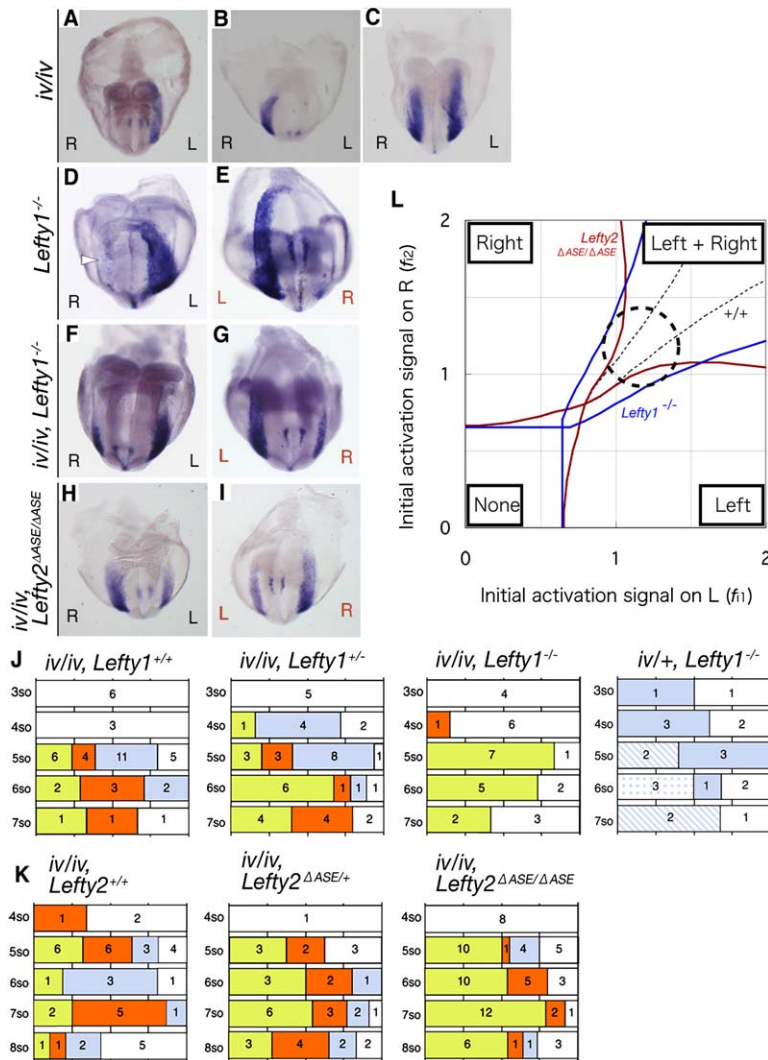


Figure 6. Roles of Lefty1 and Lefty2 in L-R Determination Mediated by the Self-Enhancement and Lateral-Inhibition System

(A–I) Representative expression patterns of *Nodal* in (A–C) *iv/iv*, (D and E) *Lefty1*<sup>-/-</sup>, (F and G) *iv/iv, Lefty1*<sup>-/-</sup>, and (H and I) *iv/iv, Lefty2*<sup>ΔASE/ΔASE</sup> mutant embryos at the five-somite stage. Anterior views are shown in (A)–(C), (D), (F), and (H); posterior views of the embryos in (D), (F), and (H) are shown in (E), (G), and (I), respectively. Expression in the LPM at the level of the node is (A) left sided, (B) right sided, or (C) bilateral in *iv/iv* embryos, (D and E) left sided in *Lefty1*<sup>-/-</sup> embryos, and predominantly bilateral in (F and G) *iv/iv, Lefty1*<sup>-/-</sup> and (H and I) *iv/iv, Lefty2*<sup>ΔASE/ΔASE</sup> embryos. The open arrowhead in (D) indicates *Nodal* expression in the anterior part of the right LPM.

(J and K) Summary of *Nodal* expression patterns in embryos of the indicated genotypes and stages. The color code is as in Figure 1I, with the addition that blue spots indicate *Nodal* expression confined to the anterior portion of the right LPM.

(L) Relationship between *Nodal* expression patterns in the LPM and  $f_1$  and  $f_2$  in *Lefty1*<sup>-/-</sup> embryos (blue lines) and *Lefty2*<sup>ΔASE/ΔASE</sup> embryos (red lines), compared to wild-type embryos (dotted, black lines). The broken circle indicates the range of  $f_1$  and  $f_2$  in *iv/iv* embryos, as in Figure 3D. For *Lefty1*<sup>-/-</sup> embryos, most of the broken circle is located in the L+R region, predicting that *Nodal* expression should be bilateral in most *iv/iv, Lefty1*<sup>-/-</sup> embryos. Similarly, the simulation predicts that the frequency of bilateral *Nodal* expression should be greater for *iv/iv, Lefty2*<sup>ΔASE/ΔASE</sup> embryos than for *iv/iv* embryos.

LPM as well as at a lower level in the right LPM (four-somite stage, 5/5 specimens; five-somite stage, 3/6 specimens). Finally, at the six-somite stage, *Nodal* mRNA was present in the left LPM, but absent in almost all (4/5) specimens of the right LPM.

In contrast, *Lefty2* mRNA was not detected by RT-PCR in the right LPM of almost all embryos examined (Figures 7C and 7D). Such an outcome was predicted because expression of *Lefty2* requires a higher level of the *Nodal* signal than does *Nodal* expression. The absence of *Lefty2* mRNA in most of the specimens of the right LPM also confirms the absence of crosscontamination between the left and right LPM. These results indicate that *Nodal* expression is indeed initiated in the right LPM by the activating signal, but that it is rapidly terminated as a result of long-range inhibition from the left LPM and midline.

## Discussion

### Nodal and Lefty Constitute a Self-Enhancement and Lateral-Inhibition System

*Nodal* and *Lefty* proteins are able to diffuse and act over long distances in the zebrafish embryo (Chen and

Schier, 2001, 2002) as well as in the mouse embryo (Meno et al., 2001; Sakuma et al., 2002). Our present results (such as the observation that *Lefty* produced in the right LPM is able to inhibit *Nodal* expression on the opposite side) also support this notion. *Nodal* and *Lefty* thus appear to fulfill one of the requirements for players in a SELI system and to perform L-R determination by using the SELI system. However, the most important requirement is that the inhibitor (*Lefty*) activity spreads farther than the activator (*Nodal*) activity, which is essential to repress *Nodal* expression on the opposite side. Our previous (Sakuma et al., 2002) and present observations suggest that *Lefty* activity indeed spreads farther than that of *Nodal*. To confirm this finding, however, it will be necessary to visualize diffusing *Nodal* and *Lefty* proteins directly in living mouse embryos, a feat that has not been possible because of technical difficulties.

Two *Lefty* genes (*Lefty1* and *Lefty2*) have been identified in mouse, and the products of both of these genes appear to be components of the SELI system. At the level of the node, *Lefty1* is expressed at the midline, whereas *Lefty2* is expressed in the left LPM and at the midline (*Lefty1* is also expressed in the left LPM, but only in the anterior portion) (Meno et al., 1998). Although

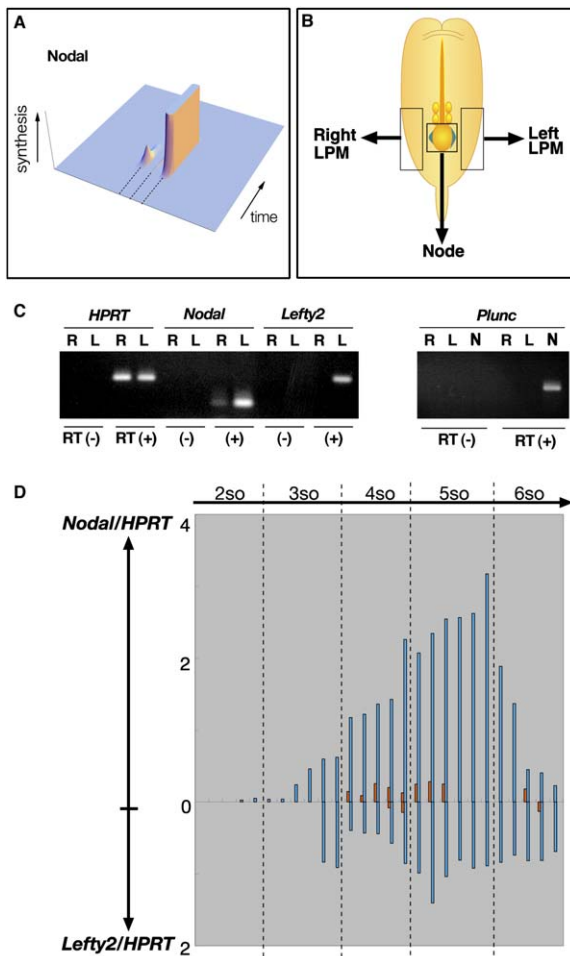


**Figure 7. *Nodal* Expression Occurs at a Low Level in the Right LPM**  
 (A) Mathematical simulation of *Nodal* expression in the wild-type embryo. The scale of the synthesis axis is 40-fold magnified compared to Figure 3F. It should be noted that a low level of *Nodal* is transiently produced in the right LPM.  
 (B) Experimental strategy for RT-PCR experiments. Pieces of the right and left LPM at the level of the node were dissected from mouse embryos at the two- to six-somite stages.  
 (C) RT-PCR analysis of *HPRT*, *Nodal*, *Lefty2*, and *L-Plunc* expression. Representative results for the right LPM (R), the left LPM (L), and the node (N) of an embryo at the four-somite stage are shown. Reactions were performed with or without reverse transcriptase (RT(+)) or RT(-), respectively). The *Nodal* product was detected in the left and right LPM, whereas the *Lefty2* product was detected only in the left LPM.  
 (D) Summary of the RT-PCR data obtained from 27 embryos between the two- and six-somite stages. Each bar indicates the intensity of the PCR product for *Nodal* or *Lefty2* normalized by that of the product for *HPRT*. The same set of RNA samples was used for analysis of each gene. Red and blue bars indicate samples from the right and left LPM, respectively.

both *Lefty* proteins are required to generate robust L-R asymmetry, the contribution of *Lefty1* seems to be larger than that of *Lefty2*, as evidenced by the comparison of *iv/iv*, *Lefty1*<sup>-/-</sup> embryos with *iv/iv*, *Lefty2*<sup>ΔASE/ΔASE</sup> embryos. Similarly, our theoretical model predicts that *Lefty* at the midline contributes more than that in the left LPM (Figure 6L), possibly because the midline is closer to the right LPM than is the left LPM. The important role of the midline was previously predicted (Danos

and Yost, 1996; Meinhardt and Gierer, 2000; Meno et al., 1998).

### The Mathematical Model Not Only Simulates but Also Predicts and Explains Certain Phenotypes

Our mathematical model was constructed on the basis of the principle proposed by Meinhardt and Gierer (2000). The model can simulate dynamic expression patterns of *Nodal* and *Lefty* in the wild-type and various mutant mice. The model contains more than 30 parameters, among which the diffusion rates are important parameters. The diffusion velocity, abundance, and functional range of Decapentaplegic, a member of the TGF-β family of proteins, in the *Drosophila* embryo appear to be regulated by various mechanisms mediated by endocytosis, argosomes, and heparan sulfate proteoglycans (Belenkaya et al., 2004; Entchev et al., 2000; Greco et al., 2001; Panakova et al., 2005). It is likely that the diffusion rates of *Nodal* and *Lefty* proteins in the mouse embryo are precisely controlled by similar mechanisms.

It is not possible to measure the exact values of the parameters included in our mathematical model. In addition, we do not know the precise level (number of molecules per cell) of the various mRNAs or proteins. Nonetheless, our model is able to simulate the dynamic expression patterns of *Nodal*, *Lefty1*, *Lefty2*, and *Pitx2* in the wild-type mouse embryo. Even the small difference in timing between *Nodal* expression and *Lefty* expression is recapitulated; *Nodal* expression begins and disappears earlier than that of *Lefty2*. Furthermore, our RT-PCR data showing that *Nodal* expression in the right LPM begins later and disappears earlier than that in the left LPM are consistent with the simulation. The model also simulates the aberrant expression patterns of *Nodal*, *Lefty1*, and *Lefty2* in all available L-R patterning mutants, including those with impaired intraflagellar transport. Furthermore, it can predict the phenotype of new mutants, as evidenced by the *iv*, *Lefty* double mutants. Finally, the model provides a mechanistic basis for observed phenotypes that are otherwise difficult to explain, as exemplified by that of *Foxh1* conditional knockout mice.

### Conversion of a Small L-R Difference into Robust Asymmetry by the Self-Enhancement and Lateral-Inhibition System

Although it remains to be determined how an asymmetric signal is transferred from the node to the LPM, several recent lines of evidence support the notion that *Nodal* protein produced in the node may migrate to the LPM, where it activates expression of the *Nodal* gene (Brennan et al., 2002; Saijoh et al., 2003, 2005). If this is the case, the initial activating signal ( $f_i$ ) in our model would be the level of *Nodal* activity that reaches the LPM from the node. It is likely that a difference in  $f_i$  between the left and right sides of the LPM is generated by nodal flow, with the higher level being achieved on the left side. Our model suggests that a small difference in  $f_i$  (such as 1.5 versus 1.0 for the left and right sides, respectively) would be sufficient to generate asymmetric gene expression. The magnitude of the difference in vivo is unknown, but our data obtained by induction of left-sided expression of EGFP-*Lefty2* show that the right side does receive an activating signal. Several genes

expressed in the perinodal region (*Nodal*, *Cer2*, *Plunc*) (Collignon et al., 1996; Hou et al., 2004; Pearce et al., 1999) exhibit a subtle L-R asymmetry in their expression patterns, possibly reflecting the initial L-R difference in the level of the activating signal in our model.

*Nodal* flow is most likely the L-R symmetry-breaking event, at least in the mouse, although there is some controversy (see a review by Tabin, [2005]). However, our data suggest that this flow alone does not generate robust asymmetry. Instead, the flow itself likely generates a relatively subtle asymmetry between the two sides. Thus, only bilateral gene expression would be generated without a SELI system. This notion is supported by our observations that suppression of the left side results in activation of the right side, and that a low level of *Nodal* expression is initiated early on the right side. *Nodal* flow was recently observed in zebrafish, rabbit, and medaka fish embryos (Essner et al., 2005; Okada et al., 2005), suggesting that it may be a conserved mechanism among vertebrates. A combination of nodal flow and a SELI system may thus also be a conserved mechanism for generation of robust asymmetry in vertebrates.

#### Experimental Procedures

##### Mice

*Lefty1*<sup>-/-</sup> and *Lefty2*<sup>ΔASE/ΔASE</sup> mice have been described previously (Meno et al., 1998, 2001). To generate *iv/iv*, *Lefty1*<sup>-/-</sup> and *iv/iv*, *Lefty2*<sup>ΔASE/ΔASE</sup> double mutants, we crossed *Lefty1*<sup>+/-</sup> or *Lefty2*<sup>+/-</sup> mice with *iv/iv* mice (Supp et al., 1997).

**Introduction of Expression Vectors into the LPM or the Yolk Sac**  
E8.0 embryos were dissected from the uterus, and the parietal endoderm membrane was removed. Expression vectors for EGFP, *Nodal*, or *Lefty* were introduced into the LPM or the yolk sac with the use of a Narishige injector. Liposomes composed of expression vectors and Lipofectamine 2000 (Invitrogen) were injected between the endoderm and the LPM with an injection pipette as described previously (Yamamoto et al., 2004). Embryos were cultured with rotation for 12 or 16 hr under a humidified atmosphere of 5% CO<sub>2</sub> at 37°C in a Falcon tube containing Dulbecco's modified Eagle's medium supplemented with 75% rat serum. They were examined with a Leica compound fluorescence microscope equipped with GFP2 optics. Embryos in which EGFP expression was apparent in the desired regions were selected for whole-mount in situ hybridization. ICR mice were used for the lipofection, LPM explant culture, and RT-PCR experiments, with the exception that B6/129 mice were used for the experiments shown in Figure 2.

##### Culture of Dissected Explants of the Right LPM

The right LPM with or without the node was dissected from ICR mouse embryos at the two-somite stage; the midline was not included. Dissected explants were cultured for 6 hr under the same conditions as those described above, with the exception that explants were cultured in static dishes. After culture, the explants were fixed and subjected to whole-mount in situ hybridization.

##### Whole-Mount In Situ Hybridization

Whole-mount in situ hybridization was performed according to standard procedures. Two-color whole-mount in situ hybridization was performed as described previously (Yamamoto et al., 2004).

##### RT-PCR

A piece of the right or left LPM at the level of the node was dissected from ICR embryos (Figure 7B), and total RNA was prepared from the tissue with the use of a ChargeSwitch Kit (Invitrogen). The volumes of reagents predetermined in the kit were scaled down for the LPM specimens. The RT reaction and PCR were performed with the use of Ready-To-Go RT-PCR beads (Amersham BioSciences). Each sample was analyzed with four sets of primers. The *HPRT*

primers were described previously (Morgan et al., 1998), the *Nodal* primers were 5'-TACCAACCATGCCTACATCCAG-3' and 5'-TCTGT CAGAGGCACCCACACTC-3', the *Lefty2* primers were 5'-TCACCA TTGAATGGCTGAGAGTC-3' and 5'-GTGCCTTCAGTCACTGGTACC TCG-3', and the *L-Plunc* primers were 5'-AGGCAGCCAACAAGCT GGGG-3' and 5'-GGAGGAGGCTGGAGTGAGCTT-3'. Each primer pair was designed to span an intron, making it possible to distinguish PCR products generated from cDNA and those derived from genomic DNA. Each PCR cycle comprised incubations at 95°C for 30 s, the annealing temperature for 30 s, and 72°C for 30 s. The annealing temperature was 60°, 62°, 60°, or 63°C for *HPRT*, *Nodal*, *Lefty2*, and *L-Plunc*, respectively, and PCR was performed for 31, 39, 39, or 46 cycles, respectively. The intensity of ethidium bromide-stained bands corresponding to each PCR product in the gel was measured with Adobe Photoshop CS2 software. The amount of PCR products for *Nodal* and *Lefty2* was normalized by that of the product for *HPRT*.

##### Mathematical Simulation

We constructed a mathematical model based on the SELI system with the use of MATHEMATICA (ver. 5.0.1) software (Wolfram Media). The model includes three partial differential equations for three components (*Nodal*, *Lefty*, and *Pitx2*). It is based on the principle proposed by Turing (1952) and Meinhardt and Gierer (2000). The mathematical equations are presented in the Supplemental Data.

##### Supplemental Data

Supplemental Data include six figures, one table, and supplemental text on the mathematical model and simulation and are available at <http://www.developmentalcell.com/cgi/content/full/11/4/495/DC1/>.

##### Acknowledgments

This work was supported by grants from the Ministry of Education, Culture, Sports, Science, and Technology of Japan and by Core Research for Evolutional Science and Technology (CREST), Japan Science and Technology Corporation (JST). We thank H. Meinhardt and S. Kondo for discussion on the R-D system, as well as K. Yamashita and S. Ohishi for technical assistance.

Received: March 8, 2006

Revised: May 1, 2006

Accepted: August 8, 2006

Published: October 2, 2006

##### References

- Asai, R., Taguchi, E., Kume, Y., Saito, M., and Kondo, S. (1999). Zebrafish leopard gene as a component of the putative reaction-diffusion system. *Mech. Dev.* 89, 87–92.
- Belenkaya, T.Y., Han, C., Yan, D., Opoka, R.J., Khodoun, M., Liu, H., and Lin, X. (2004). *Drosophila* Dpp morphogen movement is independent of dynamin-mediated endocytosis but regulated by the glycan members of heparan sulfate proteoglycans. *Cell* 119, 231–244.
- Brennan, J., Norris, D.P., and Robertson, E.J. (2002). Nodal activity in the node governs left-right asymmetry. *Genes Dev.* 16, 2339–2344.
- Chen, Y., and Schier, A.F. (2001). The zebrafish *Nodal* signal Squint functions as a morphogen. *Nature* 411, 607–610.
- Chen, Y., and Schier, A.F. (2002). Lefty proteins are long-range inhibitors of squint-mediated nodal signaling. *Curr. Biol.* 12, 2124–2128.
- Collignon, J., Varlet, I., and Robertson, E.J. (1996). Relationship between asymmetric nodal expression and the direction of embryonic turning. *Nature* 381, 155–158.
- Danos, M.C., and Yost, H.J. (1996). Role of notochord in specification of cardiac left-right orientation in zebrafish and *Xenopus*. *Dev. Biol.* 177, 96–103.
- Entchev, E.V., Schwabedissen, A., and Gonzalez-Gaitan, M. (2000). Gradient formation of the TGF-β homolog Dpp. *Cell* 103, 981–991.
- Essner, J.J., Amack, J.D., Nyholm, M.K., Harris, E.B., and Yost, H.J. (2005). Kupffer's vesicle is a ciliated organ of asymmetry in the

- zebrafish embryo that initiates left-right development of the brain, heart and gut. *Development* 132, 1247–1260.
- Greco, V., Hannus, M., and Eaton, S. (2001). Argosomes: a potential vehicle for the spread of morphogens through epithelia. *Cell* 106, 633–645.
- Hamada, H., Meno, C., Watanabe, D., and Saijoh, Y. (2002). Establishment of vertebrate left-right asymmetry. *Nat. Rev. Genet.* 3, 103–113.
- Hou, J., Yashiro, K., Okazaki, Y., Saijoh, Y., Hayashizaki, Y., and Hamada, H. (2004). Identification of a novel left-right asymmetrically expressed gene in the mouse belonging to the BPI/PLUNC superfamily. *Dev. Dyn.* 229, 373–379.
- Huangfu, D., Liu, A., Rakeman, A.S., Murcia, N.S., Niswander, L., and Anderson, K.V. (2003). Hedgehog signalling in the mouse requires intraflagellar transport proteins. *Nature* 426, 83–87.
- Juan, H., and Hamada, H. (2001). Roles of nodal-lefty regulatory loops in embryonic patterning of vertebrates. *Genes Cells* 6, 923–930.
- Kondo, S. (2002). The reaction-diffusion system: a mechanism for autonomous pattern formation in the animal skin. *Genes Cells* 7, 535–541.
- Lee, H.X., Ambrosio, A.L., Reversade, B., and De Robertis, E.D. (2006). Embryonic dorsal-ventral signaling: secreted frizzled-related proteins as inhibitors of tolloid proteinases. *Cell* 124, 147–159.
- Levin, M. (2005). Left-right asymmetry in embryonic development: a comprehensive review. *Mech. Dev.* 122, 3–25.
- Lowe, L.A., Supp, D.M., Sampath, K., Yokoyama, T., Wright, C.V., Potter, S.S., Overbeek, P., and Kuehn, M.R. (1996). Conserved left-right asymmetry of nodal expression and alterations in murine situs inversus. *Nature* 381, 158–161.
- Meinhardt, H. (2001). Organizer and axes formation as a self-organizing process. *Int. J. Dev. Biol.* 45, 177–188.
- Meinhardt, H., and Gierer, A. (2000). Pattern formation by local self-activation and lateral inhibition. *Bioessays* 22, 753–760.
- Meno, C., Shimono, A., Saijoh, Y., Yashiro, K., Mochida, K., Ohishi, S., Noji, S., Kondoh, H., and Hamada, H. (1998). *lefty-1* is required for left-right determination as a regulator of *lefty-2* and nodal. *Cell* 94, 287–297.
- Meno, C., Takeuchi, J., Sakuma, R., Koshiba-Takeuchi, K., Ohishi, S., Saijoh, Y., Miyazaki, J., ten Dijke, P., Ogura, T., and Hamada, H. (2001). Diffusion of nodal signaling activity in the absence of the feedback inhibitor *Lefty2*. *Dev. Cell* 1, 127–138.
- Morgan, D., Tumpenny, L., Goodship, J., Dai, W., Majumder, K., Matthews, L., Gardner, A., Schuster, G., Vien, L., Harrison, W., et al. (1998). *Inversin*, a novel gene in the vertebrate left-right axis pathway, is partially deleted in the *inv* mouse. *Nat. Genet.* 20, 149–156.
- Murcia, N.S., Richards, W.G., Yoder, B.K., Mucenski, M.L., Dunlap, J.R., and Woychik, R.P. (2000). The Oak Ridge Polycystic Kidney (*ork*) disease gene is required for left-right axis determination. *Development* 127, 2347–2355.
- Nonaka, S., Tanaka, Y., Okada, Y., Takeda, S., Harada, A., Kanai, Y., Kido, M., and Hirokawa, N. (1998). Randomization of left-right asymmetry due to loss of nodal cilia generating leftward flow of extraembryonic fluid in mice lacking KIF3B motor protein. *Cell* 95, 829–837.
- Okada, Y., Nonaka, S., Tanaka, Y., Saijoh, Y., Hamada, H., and Hirokawa, N. (1999). Abnormal nodal flow precedes situs inversus in *iv* and *inv* mice. *Mol. Cell* 4, 459–468.
- Okada, Y., Takeda, S., Tanaka, Y., Belmonte, J.C., and Hirokawa, N. (2005). Mechanism of nodal flow: a conserved symmetry breaking event in left-right axis determination. *Cell* 121, 633–644.
- Panakova, D., Sprong, H., Marois, E., Thiele, C., and Eaton, S. (2005). Lipoprotein particles are required for Hedgehog and Wingless signalling. *Nature* 435, 58–65.
- Pearce, J.J., Penny, G., and Rossant, J. (1999). A mouse cerberus/*Dan*-related gene family. *Dev. Biol.* 209, 98–110.
- Saijoh, Y., Adachi, H., Sakuma, R., Yeo, C.Y., Yashiro, K., Watanabe, M., Hashiguchi, H., Mochida, K., Ohishi, S., Kawabata, M., et al. (2000). Left-right asymmetric expression of *lefty2* and nodal is induced by a signaling pathway that includes the transcription factor FAST2. *Mol. Cell* 5, 35–47.
- Saijoh, Y., Oki, S., Ohishi, S., and Hamada, H. (2003). Left-right patterning of the mouse lateral plate requires nodal produced in the node. *Dev. Biol.* 256, 160–172.
- Saijoh, Y., Oki, S., Tanaka, C., Nakamura, T., Adachi, H., Yan, Y.T., Shen, M.M., and Hamada, H. (2005). Two nodal-responsive enhancers control left-right asymmetric expression of Nodal. *Dev. Dyn.* 232, 1031–1036.
- Sakuma, R., Ohnishi Yi, Y., Meno, C., Fujii, H., Juan, H., Takeuchi, J., Ogura, T., Li, E., Miyazono, K., and Hamada, H. (2002). Inhibition of Nodal signalling by *Lefty* mediated through interaction with common receptors and efficient diffusion. *Genes Cells* 7, 401–412.
- Shiratori, H., Sakuma, R., Watanabe, M., Hashiguchi, H., Mochida, K., Sakai, Y., Nishino, J., Saijoh, Y., Whitman, M., and Hamada, H. (2001). Two-step regulation of left-right asymmetric expression of *Pitx2*: initiation by nodal signaling and maintenance by *Nkx2*. *Mol. Cell* 7, 137–149.
- Supp, D.M., Witte, D.P., Potter, S.S., and Brueckner, M. (1997). Mutation of an axonemal dynein affects left-right asymmetry in *inversus viscerum* mice. *Nature* 389, 963–966.
- Tabin, C. (2005). Do we know anything about how left-right asymmetry is first established in the vertebrate embryo? *J. Mol. Histol.* 36, 317–323.
- Turing, A.M. (1952). The chemical basis of morphogenesis. *Philos. Trans. R. Soc. Lond. B Biol. Sci.* B237, 37–72.
- Whitman, M. (1998). Smads and early developmental signaling by the TGF $\beta$  superfamily. *Genes Dev.* 12, 2445–2462.
- Yamamoto, M., Mine, N., Mochida, K., Sakai, Y., Saijoh, Y., Meno, C., and Hamada, H. (2003). Nodal signaling induces the midline barrier by activating Nodal expression in the lateral plate. *Development* 130, 1795–1804.
- Yamamoto, M., Saijoh, Y., Perea-Gomez, A., Shawlot, W., Behringer, R.R., Ang, S.L., Hamada, H., and Meno, C. (2004). Nodal antagonists regulate formation of the anteroposterior axis of the mouse embryo. *Nature* 428, 387–392.